



NJC

**Preparation of Mg, Ca, or Sr-included mesoporous silica  
from glass bottle waste for recovery of rare earth metal  
elements**

Journal:	<i>New Journal of Chemistry</i>
Manuscript ID	NJ-ART-01-2024-000043.R1
Article Type:	Paper
Date Submitted by the Author:	19-Feb-2024
Complete List of Authors:	Takei, Takahiro; University of Yamanashi, Center for Crystal Science and Technology Takimoto, Kousuke; University of Yamanashi Takabayashi, Tomohiro; University of Yamanashi Saito, Norio; University of Yamanashi, Center for Crystal Science and Technolog Kumada, Nobuhiro; University of Yamanashi, Center for Crystal Science and Technology

SCHOLARONE™  
Manuscripts

## ARTICLE

# Preparation of Mg, Ca, or Sr-included mesoporous silica from glass bottle waste for recovery of rare earth metal elements

Takahiro Takei,\* Kousuke Takimoto, Tomohiro Takabayashi, Norio Saito and Nobuhiro Kumada

Received 00th January 20xx,  
Accepted 00th January 20xx

DOI: 10.1039/x0xx00000x

Mesoporous silica–alkali earth (Mg, Ca, or Sr) hybrids were prepared from waste glass as a silica source. The mesoporous silica containing no alkali earth succeeded in preparing a perfect pore structure arranged hexagonally. On increasing alkali earth element, the mesoporous structures are preserved on a small amount of the alkali-earth element as a substituent and tend to diminish with an increase of the substituent to reduce the surface area. We examined the scale-up experiment for the production of a large amount of hybrids. The scale-up system factor we proposed was relatively small, indicating relatively high production efficiency. Besides, the hybrids were examined for the ion-exchangeability of rare-earth metals. The tendency of the amount for ion-exchange showed a positive convex tetrad effect, which means a decrease in the ionicity of the rare-earth metals during an exchange. Since XANES spectra confirm the trivalent state of each rare-earth metal in the ion-exchanged hybrids, the rare-earth metals are found to exchange from the alkali-earth elements because the exchanged amount is 2/3 of the alkali-earth element leached.

## 1. Introduction

Recently, most of the wastes from glass bottles with normal colors such as brown, green, and no shade, are almost completely treated by recycling in the industrial cycle.<sup>1</sup> However, the bottle with special color, ex. red, blue, pink, black, and so on, were difficult to recycle because the amount of these bottles with special color is much smaller than those with normal color. Since the amount of specially colored glass waste is much smaller than the amount of the others, the recovery is performed by which an economical advantage can be made. Thus, bottles with unique colors cannot be recovered for each color, and they are generally gathered together. For such reasons, new processes should be developed for the application of the glass cullet with a mixed unique color.

The glass cullet has a stable chemical composition because of the industrial material. We reported the formation of porous materials from the glass cullet with special colors.<sup>2</sup> In the paper, the porous materials were reported to be prepared by hydrothermal reaction with stirring during the reaction. In these reactions, silica components were leached by alkali and the remainder became to form the porous body. Whereas at this time, we will be focusing on the leached silica solution. The main components of the leached silica solution may be composed of silica and alkali, and some impurities such as alumina, calcia, and other metal oxides may be also contained.

In these components in this solution, silica is acidic and the other components have basic properties. Since this solution will have a strong basic property, only silica may deposit by adjusting the pH value. From these considerations, the solution can be a candidate for an environmentally friendly silica source. In this paper, we are considering the application of the silica source from the colored bottle glass waste for the preparation of mesoporous silica (MPS).

MPS with hexagonal pore array is widely examined for adsorbent, catalyst support, molecular sieve, and so on.<sup>3–5</sup> The pore wall of the MPS is generally amorphous silica, and it is flexible for the incorporation of secondary components as follows. Many researchers have reported that other elements can be added to the silica network for an application for a heterogeneous catalyst by emphasis on solid acidity.<sup>6–9</sup> Some researchers have also reported a similar catalyst by solid base<sup>10,11</sup> or by bimetallic silicate.<sup>12,13</sup> Besides, we have reported that alkali-earth metals have been incorporated into the MPS network to invest in ion-exchangeability.<sup>14</sup> In these materials, XPS spectra confirm that around less than 40 mol% of the alkali-earth cation was dispersed relatively well. For the MPS-hybrid, tetraethoxysilane (TEOS) was used as a silica source, which had hydrophobic characteristics before the hydrolysis reaction. Alkali-earth nitrate salts used for the raw materials will be difficult to mix with silica until the hydrolysis of the TEOS. Thus, the leached silica solution from the waste glass may be better than TEOS as a silica source for the preparation of MPS with a metallosilicate wall. Besides, the leached silica solution has an apparent advantage compared to the TEOS in the view of cost; The silica source from the waste glass was cheaper than the TEOS. The low cost can be a good affection for the futural industrial manufacturing.

Center for Crystal Science and Technology, University of Yamanashi, 7-32 Miyamae, Kofu, Yamanashi 400-0021, Japan. E-mail: takei@yamanashi.ac.jp

† Footnotes relating to the title and/or authors should appear here.

Electronic Supplementary Information (ESI) available: [details of any supplementary information available should be included here]. See DOI: 10.1039/x0xx00000x

As mentioned before, the MPS composed of a metallosilicate wall with alkali-earth can be used for ion-exchange reaction from our report.<sup>14</sup> In this literature, the alkali-earth metallosilicate MPS has competency for ion-exchange with rare-earth metals. The rare-earth metal can be used for luminescence, magnetic, laser materials, etc. which can support our lives.<sup>15,16</sup> The distribution of the rare earth elements in the earth's crust is inhomogeneous, and recycling the rare earth elements in the electric equipment trash and/or urban mines is one of the important techniques for preserving the earth's environment, which will lead to SDGs.<sup>17</sup> In this paper, we will investigate the preparation of the MPS/alkali-earth hybrid from the waste glass, and examine its ion-exchangeability for the rare-earth metals. In other words, we are confident that this research is a very promising method that combines two sustainable activities: recycling colored waste bottle glass and recovering rare earths. Besides, the mass synthesis of MPS hybrid using waste glass is also examined.

## 2. Results and discussion

### 2.1 Leaching waste glass and chemical composition of the filtrate solution

Figure 1 shows photographs of two types of waste glass cullets classified by the sieve. First, the chemical composition of the waste glass was measured by XRF, and found to be 71.4 mol% SiO<sub>2</sub>, 12.3 mol% Na<sub>2</sub>O, 12.5 mol% CaO, 1.7 mol% Al<sub>2</sub>O<sub>3</sub>, 1.2 mol% MgO, and 0.9 mol% K<sub>2</sub>O.

Figure 2 shows the relationships between the hydrothermal period and their mass losses in the 2.0 mol/L NaOH aqueous solution. The empty and filled marks mean the waste glass of WGS and WGL, respectively. The triangle and circle mean the treatment with stirring and without stirring, respectively. The mass losses may be directly related to the leaching degree. From these plots, in the case of treatment without stirring, WGL cannot be reacted due to too large a particle, whereas WGS can be leached well. In this case, a long period of around 70 hours is necessary for good leaching. On the other hand, the hydrothermal treatment with stirring accelerates the reaction drastically even for WGL. Under stirring circumstances, the leaching degree of the WGL increases steeply and shows a plateau at around 20 hours or longer.

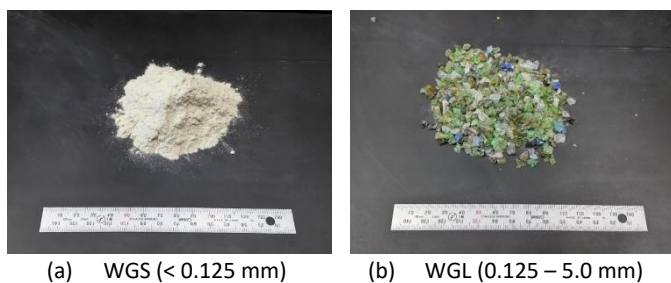


Figure 1. Photograph of the waste glass; (a) WGS and (b) WGL.

Since the rate of leaching WGL increased surprisingly by stirring during hydrothermal treatment. From this result, there

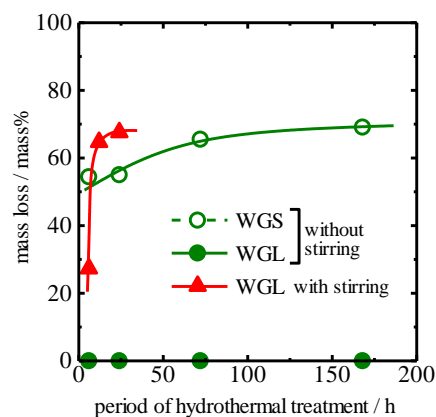


Figure 2. Relationships between hydrothermal period and their mass losses of the waste glass in the 2.0 mol/L NaOH aqueous solution.

is no reason for the unuse of the stirring process for the leaching treatment. The resultant aqueous solution was examined for chemical composition by ICP, and the solution was found to contain SiO<sub>2</sub>, Na<sub>2</sub>O, and Al<sub>2</sub>O<sub>3</sub> at 1.49, 1.15, and 0.02 mol/L, respectively. Hereafter, the aqueous solution produced from the process by which the hydrothermal treatment was performed with stirring for 24 hours was used for further experiments.

### 2.2 Preparation of MPS hybrid from the waste glass and its structural estimation

Figure 3 shows the amount of alkali-earth elements in the MPS-M20 with changing pH values in preparation. From these tendencies, Ca and Sr tend to increase in pH. However, the amount of Mg shows a plateau in the range above the pH of 10. Generally, a small amount of CO<sub>2</sub> is dissolved in water, which hydrates partially to form H<sub>2</sub>CO<sub>3</sub>. A small fraction of H<sub>2</sub>CO<sub>3</sub> dissociates to generate HCO<sub>3</sub><sup>-</sup> and CO<sub>3</sub><sup>2-</sup>. The CO<sub>3</sub><sup>2-</sup> concentration increases on the increase of pH according to Le Chatelier's principle. Therefore, a high pH will increase carbonate salt, and we adopt a pH of 10.5 to avoid carbonate formation, hereafter.

Figure 4 shows XRD patterns of MPS hybrid with different amounts of substituents. From these patterns, the intensity of the peaks derived from hexagonal texture degrades depending on the loaded amount of the second component. The sample

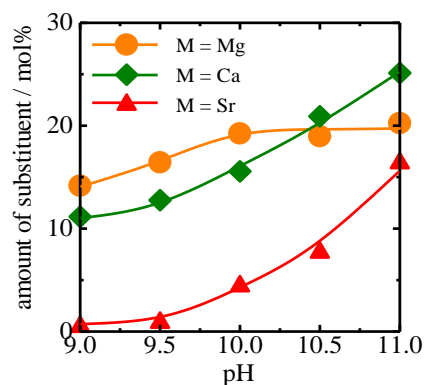
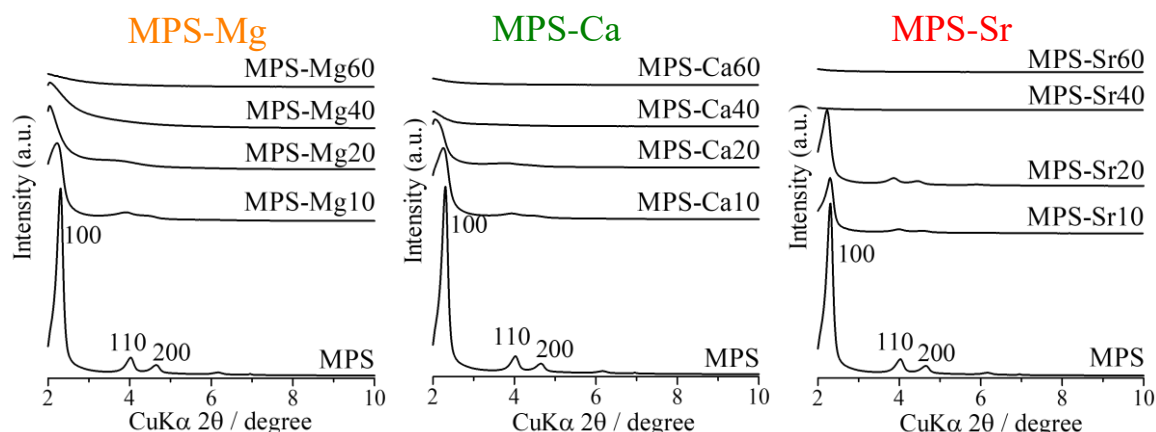


Figure 3. Amount of alkali-earth elements in the MPS-M20 with changing pH values in preparation.



**Figure 4.** XRD patterns of MPS hybrid with different amounts of substituents prepared at pH of 10.5.

with 40% or above cannot show the diffraction line meaning 100 Miller plane of pore array. Such a tendency indicates that the second component decreases the crystallinity of the CTA<sup>+</sup> micelle. On the other hand, the substituent less than 20 mol% may provide a somewhat small effect on the collapse of the porous structure. Figure S1 shows the XRD patterns of MPS, MPS-Mg20, MPS-Ca20, and MPS-Sr20 prepared at pH of 10.5 on logarithmic 2θ in an electronic supplementary information (ESI). From these wide range patterns, very small amounts of carbonate can be confirmed in only MPS-Ca20 and MPS-Sr20. From these patterns, most of the alkali-earth metal seems to be contained in the silica network because of the different halo positions from MPS without alkali-earth metals. Degrees of the existence and homogeneity of alkali metals are going to be discussed via composition mapping and MAS-NMR in the next paragraph. Figure S2 shows the relationship between the loaded amount of the alkali-earth element and the amount of contained alkali-earth element. From these plots, Mg increases linearly and Ca and Sr show saturation at above 40 mol%. Isotherms and pore size distributions were shown in Figure S3. These results seem to coincide with the crystallinity estimated

from XRD patterns. Figure 5 shows relationships between the actual amount of Mg, Ca, or Sr, and specific surface area. For all substituents, the surface areas reduce on the amounts with a linear relationship. However, the slope is different in the following order; Mg, Ca, Sr. The slope value tendency is very similar to the atomic weight. For the rule of the ionic radius ratio  $r^-/r^+$ , the coordination number may be larger for larger atomic weight in an alkali-earth column. From the literature by Sun<sup>18</sup>, the mean CNs for Mg, Ca, and Sr are 6, 8, and 8. Since the larger CN may be prone to collapsing the silica network to decrease the surface area, the tendency of the surface area can be understandable. Figure S4 shows relationships between the mass fraction of the substituent and specific surface area in the ESI. From these plots, the relationships seem to be almost linear despite substituent species. the fraction on the x-axis is calculated from atomic weight rather than molar weight; no linear correlation in the molecular weight calculation. Namely, the linear relationship implies that the substituents exist singly as a network modifier that cannot participate in the silica network.

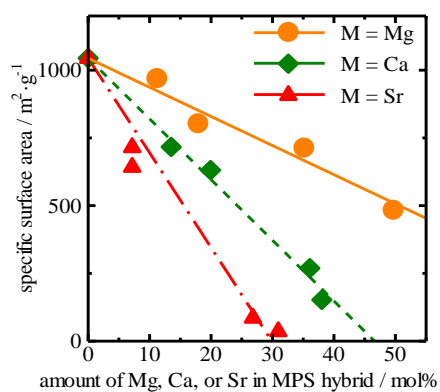


**Figure 5.** Relationships between the actual amount of Mg, Ca, or Sr, and specific surface area.

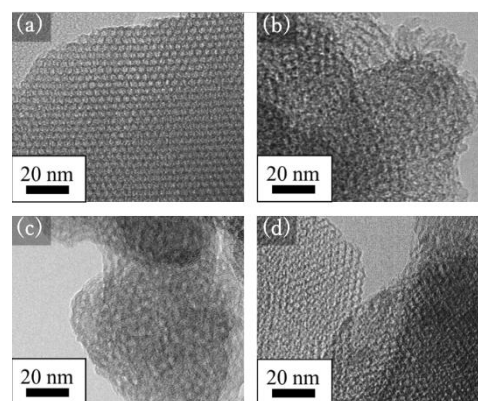


**Figure 6.** TEM photographs of MPS, MPS-Mg20, -Ca20, and -Sr20 prepared from the waste glass.

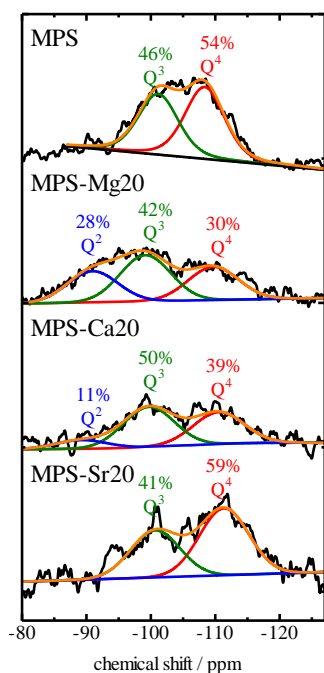


**Figure 7.**  $^{29}\text{Si}$  MAS-NMR spectra of MPS, MPS-Mg<sub>20</sub>, -Ca<sub>20</sub>, and -Sr<sub>20</sub> prepared from the waste glass with evaluated fractions of Q<sup>2</sup>, Q<sup>3</sup>, and Q<sup>4</sup>.

Figure S5 shows chemical composition mapping by SEM-EDX in the ESI. These figures confirm that the alkali-earth exists in the MPS wall homogeneously. Figure 6 shows TEM micrographs of the MPS-hybrids with 20 mol% of Mg, Ca, and Sr. The MPS without substitute appears to have a perfect pore array, though the MPS including Mg, and Ca shows mesopore texture with no periodicity. For MPS-Sr, a relative hexagonal pore array can be confirmed because the sample has a small amount of Sr (less than 10 mol%). Thus, the collapse of the pore texture may occur partially in the Sr sample. For the confirmation of the silica network in the MPS-hybrid, solid-state NMR spectra were measured. Figure 7 shows  $^{29}\text{Si}$  MAS-NMR spectra of the hybrid with evaluated fractions of Q<sup>2</sup>, Q<sup>3</sup>, and Q<sup>4</sup>. From this analysis, the Mg and Ca sample has a small amount of Q<sup>2</sup> and shows a slight decrease in Q<sup>4</sup> fraction. In the case of the Sr-sample, Q<sup>4</sup> still existed a lot. These spectra seem to be consistent with the TEM in Figure 6.

### 2.3 Scale-up effect of the MPS preparation

Figure S6 indicates a change in the specific surface area of the sample with a scale-up of the synthesis system by 10 in the ESI. From the figure, the decrease ratio in the surface area depends on the atomic mass of the substituent. On the other hand, the surface area increases slightly for the pure MPS via scaling up by 10. The reason for the decrease in the surface area is difficult to explain at first glance. The plausible reason may be the solubility and number of hydration states. In the case of the system expansion by 10 times, inhomogeneity might increase compared to the sample with no scaling-up. The 10 times scaling-up of the system was carried out by a large flask with shaking. Since the shaking conditions are the

same despite the scale, only the same energy can be given to the system. The given energy may not be enough to be perfectly homogeneous for the scaled-up system. Besides, the scale-up effect cannot be ignored. Generally, the scale-up effect can be observed when the system temperature is elevated for the following reasons. Thermal conduction will occur through the interface between the vessel and the sample solution. Usually, a large vessel has a small interface area per volume of the sample solution. Total thermal conductivity, composed of the interface and the solution, will affect the reaction degree. Thus, the thermal conductivity of the solution including the sample may be very influential for the scale-up effect. Since the thermal conductivity of Mg, Ca, and Sr are 151, 184, and 52 W · m<sup>-1</sup> · K<sup>-1</sup> at room temperature,<sup>19</sup> the MPS-Sr hybrid will reduce its own reactivity to enlarge the scale-up effect.

Figure 8(a) shows the relationship between the scale-up ratio and the specific surface area of the MPS-Ca<sub>20</sub> hybrid. The surface area decreases with increasing the scale-up ratio with a tendency like an inverse proportion at first glance. Here, we are proposing a formula,

$$D = D_0 \cdot R^{-n} \quad (1)$$

where  $D$  is the reaction rate,  $R$  is a scale-up ratio,  $D_0$  is the reaction rate at  $R=1$ , and  $n$  is defined as the scale-up system factor that means the degree of scale-up effect. The factor should be in the range from 0 to 1. No and full scale-up effect results in the value of 0 and 1, respectively. The formula (1) can be transformed as

$$\log D = \log D_0 - n \log R \quad (2)$$

For our experiments, the specific surface area,  $S_a$ , is presumed to be regarded as the proportional factor to the reaction rate,  $D$ . Figure 8(b) shows a  $\log(R)$ – $\log(S_a)$  plot. These plots can be approximated by linear line with a slope of -0.16 and an intercept of 2.81. Then, the factor  $n$  is 0.16 which corresponds to the partial effect of the scale-up in the preparation process of the MPS-Ca hybrid.

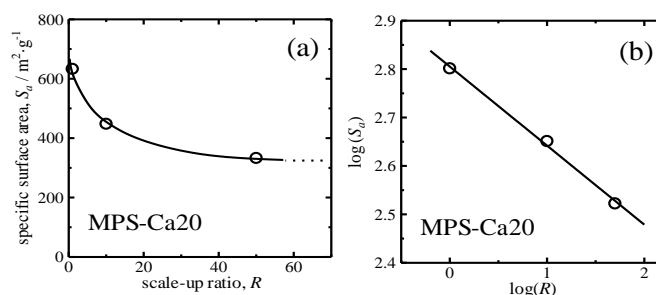


**Figure 8.** Relationship between the scale-up ratio and the specific surface area of the MPS-Ca<sub>20</sub> hybrid; (a) linear and (b) double logarithmic coordination.

### 2.4 Adsorption of the lanthanoid cations

Figure 9 shows the amount of the rare-earth metal cation-exchange versus the ionic radius of the rare-earth metal cations. For general tendencies as a first feature, four upward convexes can be observed, indicating the ionicity of the lanthanoids decreases by ion-exchange reaction from an

interpretation of the theory of the tetrad effect.<sup>20–22</sup> Such ionicity decrease may mean that the exchanged lanthanoid cation may be inserted into the silica network. The second feature is the competency of the adsorption of rare-earth metal cations in the pure MPS prepared from the waste glass. In our previous report<sup>14,23</sup>, the MPS from tetraethoxysilane with no substitution has an ignorable competency for the adsorption of rare-earth metal cations. The reason for this phenomenon of such an adsorption competency should be

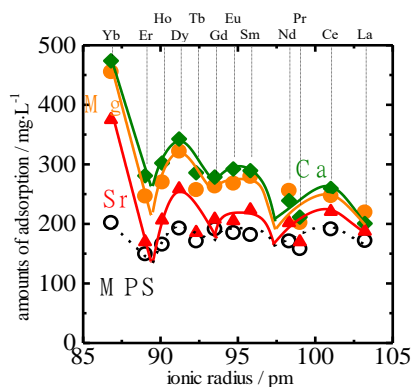


**Figure 9.** Amount of ion-exchanged rare-earth metal cations into MPS, MPS-Mg20, -Ca20, and -Sr20 prepared from the waste glass.

clear in future work.

The mechanism of rare-earth metal uptake will be investigated. First, we measured the amount of leached alkali-earth element after the treatment. In the case of MPS-Ca20, the total uptake amount of rare-earth metal is around 23.4 mmol/L and the leached amount of Ca is around 15.9 mmol/L. Then, the ratio of rare-earth metals/Ca is around 3/2. However, all rare-earth metal salts in these experiments have a trivalent state, the ratio rare-earth metals/Ca should be 2/3 if the valence of rare-earth metal cation was preserved after the ion-exchange. This discrepancy may be due to the adsorption of pure MPS produced from waste glass. Actually, the total uptake amount of rare-earth metal to the pure MPS is 12.6 mmol/L. Thus, the difference of 10.8 mmol/L between the uptake values of MPS-Ca20 and MPS is the net value by ion-exchange from Ca. Therefore, the net ratio of rare-earth metals/Ca is around 2/3, corresponding to the ion valence. The ratio can be regarded as a piece of collateral evidence for ion-exchange reactions. Incidentally, Mg and Sr including MPS show similar tendencies. (22.7 and 16.0 mmol/L of uptake amounts for MPS-Mg20 and -Sr20, respectively.) The adsorption amounts are very competitive because the past research of MPS including alkali-earth metal oxide from tetraethoxysilane shows 13, 17, and 23 mmol/L of total adsorption amount.<sup>14</sup> Thus, the total amounts seemed to be similar or better for the past research. However, the selectivity is worse than the past results. In past research, smaller ion tends to be adsorbed with higher amounts. In this research, the selectivity is not high because pure MPS from the waste glass can adsorb them for whole lanthanoids. We think the competency of the adsorption for the MPS from the waste

glass is able to be regarded as an advantage to advance the research in the future.

Besides, the chemical states of the rare-earth metals in the MPS are investigated by XAFS. Figure S7 shows XAFS spectra of lanthanoid elements in the MPS-hybrid after ion-exchange treatment in the ESI. Each spectrum was measured separately and was normalized respectively. The sample after the treatment includes many kinds of lanthanoids because of the simultaneous adsorption in the aqueous solution containing 12 sorts of lanthanoids. Each lanthanoid element has  $L_1$ ,  $L_2$ , and  $L_3$  absorption within the energy range from 5400 to 11000 eV. Therefore, the mean energy separation between neighbor  $L$ -absorption lines should be less than several hundred eV as shown in Figure S7. Generally, EXAFS can be used for the estimation of coordination state. However, the estimation is difficult for this experiment because EXAFS analysis needs at least a 700 – 800 eV range of plateau in the EXAFS area. Therefore, we use XANES spectra to consider further chemical states of the lanthanoids in MPS.

Figure 10 shows the  $L_3$  XANES spectra of the selected elements, Nd, Eu, Dy, and Yb, which have no absorption from other lanthanoids at similar or near energy. These figures include the spectrum of each lanthanoid oxide, chloride, ion-exchanged MPS-Mg20, -Ca20, and -Sr20 by each lanthanoid cation. From the absorption edge in these spectra, the lanthanoids are found to be in trivalent cationic states because of the very similar energy of the absorption edge despite sample species. In addition, all spectra of the sample in MPS-Ca or Sr show the highest white line at the absorption edge. Generally, higher ionicity provides a stronger white line in the same valent state or same coordination number for the period-6 elements including lanthanoids.<sup>24</sup> Thus, the

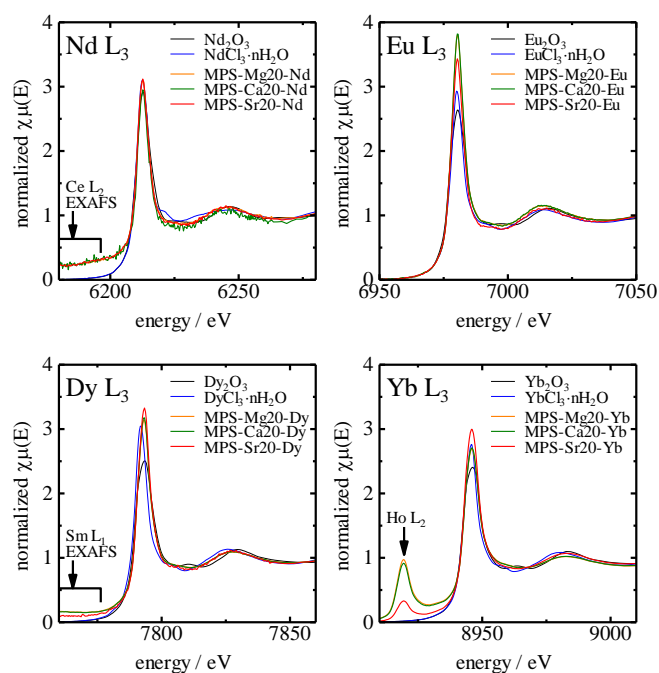


**Figure 10.**  $L_3$  XANES spectra of the selected elements, Nd, Eu, Dy, and Yb, in the ion-exchanged MPS, MPS-Mg20, -Ca20, and -Sr20 prepared from the waste glass.

lanthanoids coordinate with a relatively large amount of oxygen while keeping a trivalent state with slightly decreased ionicity.

For consideration of their reusability, the isotherms of the as-prepared and the ion-exchanged MPS-Mg20 are shown in Figure S8. The ion-exchanged MPS-Mg20 hybrid shows the capillary condensation at around 0.4 of  $P/P_0$  similar to the as prepared MPS-Mg20, but the adsorption amount decreased by the exchange. The reason for the decrease is a difference in the atomic mass between Mg and lanthanoid. Since the adsorbed amount of the rare earth metal cation is 22.7 mmol/L on the MPS-Mg20 as mentioned before, the total molecular mass should increase by 1.7 times. The increase of the total molecular mass must decrease the adsorption volume per unit mass of N<sub>2</sub>. From this result, most of the mesoporous structure is found to be retained even after the ion-exchange treatment.

### 3. Experimental

#### 3.1 Treatment of the waste bottle

A waste glass cullet of less than 5 mm in size was used as starting material. The waste glass cullet was at first classified by a 0.125 mm sieve to separate into two grades with different sizes, less than 0.125 mm and 0.125 - 5.0 mm. These two grades were designated as WGS and WGL, respectively. The classified waste bottle cullet was hydrothermally treated at 150 °C in the sodium hydroxide aqueous solution with concentrations of 2.0 mol/L similar to our previous report<sup>2</sup> for leaching silica to prepare silica-rich aq. sol. The condition of the typical process is shown as follows. 750g of the waste glass and the NaOH aqueous solution were hydrothermally treated without or with stirring at 200 rpm. After that, the reacted solution was separated by filtration. Then, the filtered aqueous solution was used as a silica source for the preparation of mesoporous silica explained in the next section.

#### 3.2 Preparation of MPS/alkali-earth hybrid

The MPS/alkali-earth hybrids were prepared as follows. The silica-containing aqueous solution obtained was used as a silica source. Hexadecylammonium bromide (CTAB) as a micelle-forming agent was dissolved completely in the 30 mL distilled water at 50 °C. After that, the silica-containing aqueous solution was put into the micelle solution with gentle stirring. Additionally, the arbitral amount of group-2 metal nitrate,  $M(\text{NO}_3)_2 \cdot n\text{H}_2\text{O}$ , was put into the solution. The ratio of Si : M : CTAB was 100-x : x : 10.5 where M was Mg, Ca, or Sr. Then, the pH value of the mixed solution was adjusted to 10.5 by HCl, and the solution was shaken or stirred at 70 °C with 200 rpm for 24 h. After the reaction, the sample was filtered and then dried at 50 °C. The dried sample was heated at 500 °C for 6 h to decompose the surfactant. The resultant samples were designated as MPS-Mx.

Preparation processes were examined to scale up to ×10 for the synthesis of MPS-M20 to investigate further industrial production. Besides, the scale-up tendency was investigated

by ×1, ×10, and ×50 for only MPS-Ca20. The experiments of the scaled-up production with ×50 were carried out by a large-scale stainless steel autoclave with a stirring screw at the same rotation rate of 200 rpm.

#### 3.1 Characterization

The silica-containing aqueous solution was diluted one thousand times and was examined for chemical composition by ICP-OES elemental analysis (SPS3520UV-DD, Hitachi high-tech Co. LTD.). The chemical composition of the prepared MPS hybrids was measured by XRF (Primus III, Rigaku) for their total composition and by SEM-EDX (Miniscope TM3030 with Quantax 70, Hitachi, Bruker) for their homogeneity. The structure of the prepared MPS hybrid was examined by XRD (MiniFlex, Rigaku) with  $\text{CuK}\alpha$  radiation, microporosimeter (BELSORP-mini, Nippon BEL), solid-state NMR (AVANCE III HD, Bruker), and XPS (Kratos, Shimadzu).

The ion-exchange properties of the hybrid, an aqueous solution with a concentration of 6 g/L including 12 rare-earth metal cations, La, Ce, Pr, Nd, Sm, Eu, Gd, Tb, Dy, Ho, Er, and Yb (500 mg/L each) was used for ion-exchange treatment. The MPS hybrid was put in the solution and then it was shaken for an arbitrary period. The concentration of the resultant solution was measured to estimate the ion-exchange capacity of the rare-earth metal by ICP-OES.

The exchanged rare-earth metal cations in the MPS hybrids were examined by XAFS (BL14B2, SPring-8). The chemical state and/or coordination state of the rare-earth metal elements were investigated via Demeter 09.26.<sup>25</sup>

### Conclusions

A waste glass cullet was used for the raw materials of the preparation of the MPS/alkali-earth hybrid. These hybrids are confirmed to have a mesoporous structure. However, these structure is prone to collapse by the substitution of silica with the alkali-earth. The arrayed pores reduced with an increase of the substituent. In the case of Sr-hybrid, the collapse degree seems to be smaller than the others in the TEM because of a smaller amount of Sr than the others in these hybrids; the Sr is difficult to include in the pore wall compared to the others as shown in Figure 3. The specific surface area tends to decrease depending on the amounts of substituent.

For the scale-up experiments, we propose the scale-up system factor,  $n$ , which expresses the effect degree of the vessel volume and somethings; the factor may contain thermal conductivity, viscosity of the solution, degree of dispersion, and so on. For reducing the factor, a solution with low viscosity and high thermal conductivity should be used. Insertion of the solid heating medium may be also effective for a decrease of the factor,  $n$ . We think the factor will be very useful for future research.

Amounts of ion-exchange of rare-earth metal were increased and a curious phenomenon emerged; the MPS without the alkali-earth element indicates a relatively large amount of uptake. Now we are analyzing the phenomenon to clarify it.

The key point is possibly the chemical composition and/or preparation pH of the MPS hybrids. We should clear the phenomenon in the futural literature. XANES spectra show at least the chemical state of exchanged lanthanoids trivalent. Besides, the tetrad effect with the four positive convex indicates a slight expansion of the f-electron like a covalent bond in the MPS network. The mechanism accelerates the uptake competency of the sample to be a strong candidate for the recovery of the rare earth cation in the future. In the manuscript, we explained that both the recycling of the colored bottle glass waste and recovery of rare earth metal cations in the aqueous solution succeeded by the preparation of alkali-earth including MPS as an ion-exchanger.

### Author Contributions

Takahiro Takei: conceptualization; investigation – experimental; writing original draft; supervision; Kousuke Takimoto: investigation – experimental; Tomohiro Takabayashi: investigation – experimental; Norio Saito: review and editing; Nobuhiro Kumada: review and editing; supervision.

### Conflicts of interest

There are no conflicts to declare.

### Acknowledgements

The experiments at SPring-8 were performed with the approval of the Japan Synchrotron Radiation Research Institute (JASRI) (Proposals 2019B1833) This work was supported by JSPS KAKENHI Grant Numbers 21K04639, and was also supported by Adaptable and Seamless Technology transfer Program through Target-driven R&D (A-STEP) from Japan Science and Technology Agency (JST) Japan Grant Number JPMJTM20DV.

### Notes and references

- J. Eid, *Nature*, 2021, **599**, 7–8.
- T. Takei, H. Ota, Q. Dong, A. Miura, Y. Yonesaki, N. Kumada and H. Takahashi, *Ceramics International*, 2012, **38**, 2153–2157.
- P. Yang, S. Gai and J. Lin, *Chem. Soc. Rev.*, 2012, **41**, 3679–3698.
- E. Yamamoto and K. Kuroda, *BCSJ*, 2016, **89**, 501–539.
- Q. Qin and Y. Xu, *Microporous and Mesoporous Materials*, 2016, **232**, 143–150.
- R. Peng, D. Zhao, N. M. Dimitrijevic, T. Rajh and R. T. Koodali, *J. Phys. Chem. C*, 2012, **116**, 1605–1613.
- T. Blasco, A. Corma, M. T. Navarro and J. P. Pariente, *Journal of Catalysis*, 1995, **156**, 65–74.
- M. T. Janicke, C. C. Landry, S. C. Christiansen, S. Birtalan, G. D. Stucky and B. F. Chmelka, *Chem. Mater.*, 1999, **11**, 1342–1351.
- X. Gao, I. E. Wachs, M. S. Wong and J. Y. Ying, *Journal of Catalysis*, 2001, **203**, 18–24.
- S.-I. Fujita, S. Segawa, K. Kawashima, X. Nie, T. Erata and M. Arai, *Journal of Materials Science & Technology*, 2018, **34**, 2521–2528.

- S. Siddiqui and Z. N. Siddiqui, *Catal Lett*, 2018, **148**, 3628–3645.
- M. Fan, S. Xu, B. An, A. M. Sheveleva, A. Betts, J. Hurd, Z. Zhu, M. He, D. Iuga, L. Lin, X. Kang, C. M. A. Parlett, F. Tuna, E. J. L. McInnes, L. L. Keenan, D. Lee, M. P. Attfield and S. Yang, *Angewandte Chemie International Edition*, 2022, **61**, e202212164.
- V. Pârvulescu, Cr. Tablet, C. Anastasescu and B. L. Su, *Catalysis Today*, 2004, **93–95**, 307–313.
- T. Takei, M. Takehara, T. Takabayashi, S. Yanagida and N. Kumada, *Colloids and Surfaces A: Physicochemical and Engineering Aspects*, 2021, **610**, 125664.
- S. Gai, C. Li, P. Yang and J. Lin, *Chem. Rev.*, 2014, **114**, 2343–2389.
- T. Dutta, K.-H. Kim, M. Uchimiya, E. E. Kwon, B.-H. Jeon, A. Deep and S.-T. Yun, *Environmental Research*, 2016, **150**, 182–190.
- M. C. Bonfante, J. P. Raspini, I. B. Fernandes, S. Fernandes, L. M. S. Campos and O. E. Alarcon, *Renewable and Sustainable Energy Reviews*, 2021, **137**, 110616.
- K.-H. Sun, *Journal of the American Ceramic Society*, 1947, **30**, 277–281.
- L. Binkle and M. Brunen, *Thermal conductivity, electrical resistivity and Lorenz function data for metallic elements in the range 273 to 1500 K*, Forschungszentrum Jülich GmbH Zentralbibliothek, Verlag, 1994.
- I. Kawabe, *Geochem. J.*, 1992, **26**, 309–335.
- I. Kawabe, *Geochem. J.*, 1999, **33**, 249–265.
- A. Ohta and I. Kawabe, *Geochim. Cosmochim. Acta*, 2001, **65**, 695–703.
- F. Okabe, C. Mochizuki, T. Takei, S. Yanagida, A. Miura and N. Kumada, *J. Ceram. Soc. Japan*, 2017, **125**, 732–736.
- H. Duggal, P. Rajput, I. Alperovich, T. Asanova, D. Mehta, S. N. Jha and S. Gautam, *Vacuum*, 2020, **176**, 109294.
- B. Ravel and M. Newville, *J Synchrotron Rad*, 2005, **12**, 537–541.